Conformationally locked lanthanide chelating tags yield one set of signals for convenient pseudocontact shift protein nuclear magnetic resonance spectroscopy: Benchmarking on ubiquitin S57C and hCA II S50C and study of the stability of the conformers by DFT calculations

Daniel Joss, MSc, Department of Chemistry, University of Basel, St. Johanns-Ring 19, CH-4056 Basel, daniel.joss@unibas.ch, ORCID 0000-0002-9101-4525

Dr. Roché M. Walliser, Department of Chemistry, University of Basel, St. Johanns-Ring 19, CH-4056 Basel, roche.walliser@gmail.com

Dr. Kaspar Zimmermann, Department of Chemistry, University of Basel, St. Johanns-Ring 19, CH-4056 Basel, zimkas00@gmail.com

PD Dr. Daniel Häussinger, NMR Laboratory, Department of Chemistry, University of Basel, St. Johanns-Ring 19, CH-4056 Basel, daniel.haeussinger@unibas.ch, ORCID 0000-0002-4798-0072

Abstract

Pseudocontact shifts (PCS) generated by lanthanide chelating tags yield valuable restraints for investigating protein structures, dynamics and interactions in solution. In this work, thulium- and dysprosium complexes of eight-fold methylated 1,4,7,10-tetraazacyclododecane-1,4,7,10-tetraacetic acid tags (DOTA-M8-(4*R*4*S*)-SSPy) are presented that induce large pseudocontact shifts up to 5.5 ppm and adopt exclusively the square antiprismatic conformation (SAP). This is in contrast to our earlier findings on tags of the stereoisomeric DOTA-M8-(8*S*)-SSPy, where significant amounts of the twisted square antiprismatic (TSAP) conformer for the Dy tag were observed.

The Dy-, Tm- and Lu complexes of DOTA-M8-(4*R*4*S*)-SSPy were conjugated to ubiquitin S57C and selectively ^{15}N leucine labeled human carbonic anhydrase II S50C, resulting in only one set of signals. Furthermore, we investigated the conformation of the lanthanide complexes in vacuo and with implicit water solvent using density functional theory calculations. The calculated energy differences between the two different conformations were determined to be in a range of 7.0 – 50.5 kJ/mol and clearly suggested a SAP ($\Lambda(\delta\delta\delta\delta)$) geometry for all investigated tags. The lanthanide chelating tags studied in this work offer insights into the solution structure of proteins by inducing strong pseudocontact shifts, show different tensor properties compared to their predecessor, enable a convenient assignment procedure, are accessed by a more economic synthesis than their predecessor and constitute a highly promising starting point for further developments of lanthanide chelating tags.

Keywords

Nuclear magnetic resonance, pseudocontact shift, lanthanide chelating tag, paramagnetic, density functional theory, protein.

Acknowledgements

The Chemistry Department of the University of Basel and the Swiss National Science Foundation grant 200021_130263 are acknowledged for financial support. Calculations were performed at sciCORE (http://scicore.unibas.ch/) scientific computing core facility at University of Basel. Biological structures were generated using the open source software PyMOL (http://www.pymol.org/). C.E. Housecroft, E.C. Constable, T. Müntener and R. Vogel are acknowledged for helpful discussions. R.A. Byrd is gratefully acknowledged for a gift of M4-cyclen.

Introduction

Pseudocontact shifts (PCS) generated by lanthanide chelating tags yield valuable restraints for investigating protein structures, dynamics and interactions in solution (Gaponenko et al. 2002; Wöhnert et al. 2003; Ikegami et al. 2004; Pintacuda et al. 2006; Keizers et al. 2008; Su et al. 2008; Häussinger et al. 2009; Su et al. 2009; Otting 2010; Peters et al. 2011; Loh et al. 2013; Liu et al. 2014; Brewer et al. 2015; Hikone et al. 2016; Müntener et al. 2016; Pan et al. 2016; Nitsche and Otting 2017). In order to access structural restraints by PCS measurements, rigidified 1,4,7,10-Tetraazacyclododecane-1,4,7,10-tetraacetic acid (DOTA)-based chelators offer a promising scaffold (Ranganathan et al. 2002; Ranganathan et al. 2002; Häussinger et al. 2009). The methyl group substituents on the nitrogen containing macrocycle adopt an equatorial-upper position (Parker et al. 2002; Opina et al. 2016) when the ligand is coordinated to a lanthanide metal ion and prevent motional averaging and line broadening of signals by locking the 12-membered ring in an (δδδδ) conformation (Häussinger et al. 2009).

However, Ln-DOTA-M8-(8*S*)-SSPy can show two signal sets, which results in a complicated analysis of spectra obtained by nuclear magnetic resonance spectroscopy containing the structural restraints for protein structure determination. As shown by Opina et al., the two signal sets have their origin in the presence of two different conformers of the lanthanide chelating tags, which can be interconverted to each other by rotation of the pendant arms of the chelator (Opina et al. 2016). In the course of their investigations, it was shown that for the Ln-DOTA-M8-(8*S*)-SSPy lanthanide chelating tags both arm rotation conformers are present in significant ratios for lanthanides heavier than europium and lighter than ytterbium and that the change in the ratio of the two possible conformers is dependent on the lanthanide ionic radii and therefore ultimately caused by the lanthanide contraction. Furthermore, it was demonstrated that the two conformers are in slow exchange on a timescale of approximately 4 h (Opina et al. 2016).

Especially for the strongly paramagnetic lanthanides dysprosium and thulium, it would be highly favorable to have only one conformational species present in rigidified DOTA-derived lanthanide chelating tags. We supposed that the pendant arms can be locked in one conformation by inverting the configuration of the stereocenter of the pendant arms (DOTA-M8-(4*R*4*S*)-SSPy), since the methyl substituents on the pendant arms would avoid steric clashes with the methyl substituents from the 12-membered ring.

Besides the locked conformation, we also expected different tensor properties compared to the DOTA-M8-(8*S*)-SSPy tag, because it was suggested by Mironov et al. that small changes in the coordination polyhedron can significantly affect the tensor properties (Mironov et al. 2001). In order to investigate this approach, we synthesized Dy-, Tm-, and Lu-DOTA-M8-(4*R*4*S*)-SSPy tags (Figure 1) and conjugated each lanthanide chelating tag to ubiquitin S57C and to leucine labeled human carbonic anhydrase II S50C protein constructs. The obtained spectra as well as tensor sizes and orientations relative to the protein were analyzed.

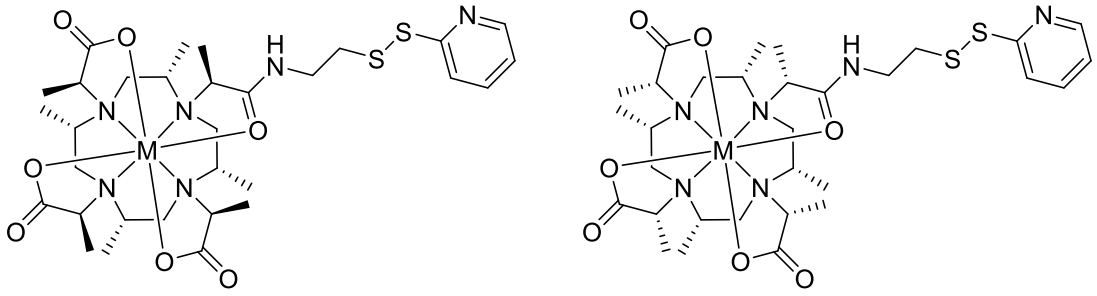

Figure 1: DOTA-M8-(8S)-SSPy (left) and DOTA-M8-(4R4S)-SSPy (right).

Density functional theory calculations were envisioned to assign the conformation of the DOTA-M8-(4*R*4*S*)-SSPy tags, since 2D NMR spectra as for example used by Ranganathan et al. for the assignment of Yb^{3+} M4-DOTMA chelates (Ranganathan et al. 2002) are difficult or even impossible to measure for the two strongly paramagnetic lanthanide chelating tags due the extremely short T2 relaxation time caused by the close paramagnetic center (Helm 2006). Density functional theory calculations gained recently attraction to study lanthanide complexes and especially their conformational behavior, since they present a highly accurate but still fast and reliable quantum mechanical approach for structure calculation of lanthanide chelating tags (Cosentino et al. 2002; Natrajan et al. 2010; Regueiro-Figueroa et al. 2011; Blahut et al. 2017). Besides the fact that suitable effective core potentials are available for the lanthanide series, e.g. the ones reported by Dolg et al. (Dolg et al. 1989; Dolg et al. 1993), the electrons can also be treated explicitly and including relativistic effects provided sufficiently powerful computational infrastructure is available. DFT calculations are an important tool for geometry optimization studies, calculation of relative energies and other molecular properties of both common organic molecules and metal complexes (Cramer and Truhlar 2009). We therefore compared the energies of SAP and TSAP geometry for the thulium and dysprosium tags and assigned the most stable conformation in aqueous solution.

Material and Methods

Synthesis

Lanthanide chelating tags were synthesized according to the procedures reported in Häussinger et al. for the Lu-DOTA-M8-(4*R*4*S*)-SSPy tag (Häussinger et al. 2009). In the amide coupling reaction, PyBOP (benzotriazol-1-yl-oxytripyrrolidinophosphonium hexafluorophosphate) was replaced by HATU (1-[Bis(dimethylamino)methylene]-1H-1,2,3-triazolo[4,5-b]pyridinium 3-oxid hexafluorophosphate) resulting in a higher yield of about 91% for this particular step in the synthesis. The side arms of DOTA-M8-(4*R*4*S*)-SSPy can conveniently be obtained from *L*-lactic acid, compared to the more expensive *D*-lactic acid needed for the synthesis of the DOTA-M8-(8*S*)-SSPy tag.

Expression of ubiquitin S57C and human carbonic anhydrase II S50C mutants and tagging reaction

Ubiquitin S57C was expressed as described previously by Sass et al., leucine labeled hCA II S50C as described by Varghese et al. (Sass et al. 1999; Varghese et al. 2016). The tagging reactions were carried out accordingly to the

procedure reported by Häussinger et al. (Häussinger et al. 2009), except that the pH during tagging was kept at pH 7.0 for ubiquitin S57C and pH 6.8 for hCA II S50C to ensure a faster tagging reaction.

NMR experiments and determination of the paramagnetic susceptibility tensor

^{1}H-^{15}N HSQC spectra were measured in 10 mM phosphate buffer with pH 6.0 (Ubiquitin S57C) and pH 6.8 (hCA II S50C) at a temperature of 298 K on a 600 MHz Bruker Avance III NMR spectrometer equipped with a cryogenic QCI probe. The obtained NMR spectra were assigned using CcpNmr Analysis (Vranken et al. 2005). The tensor properties were then obtained by fitting to the secondary structure elements of ubiquitin (PDB 1UBI (Ramage et al. 1994)) or the leucine residues of hCA II (PDB 3KS3 (Avvaru et al. 2010)) using Numbat (Schmitz et al. 2008). Q-factors were calculated using the following equation: $Q = \frac{\sqrt{\sum \left(PCS_{exp} - PCS_{calc}\right)^2}}{\sqrt{\sum \left(PCS_{exp}\right)^2}}$.

DFT calculations

DFT calculations were performed with the ORCA program package (Neese 2012) at the sciCORE facility of the University of Basel. For the calculations, BP86 was used as functional, SARC-TZVP as basis set for the ligands, while SARC2-QZVP was used as basis set for the lanthanide metal. The calculations were performed using the relativistic ZORA approximation, as well as the RI approximation to speed up the calculations. To model the water solvent, CPCM solvent model was implemented into the calculations.

Results and discussion

In order to access lanthanide chelating tags with a completely rigidified and conformationally locked scaffold that yield only one set of signals when coupled to the protein of interest and exhibit novel tensor properties, we inverted the stereochemistry of the pendant arms of the DOTA-M8-(8*S*)-SSPy tag giving DOTA-M8-(4*R*4*S*)-SSPy. The previous findings by Opina et al. (Opina et al. 2016), i.e. the formation of two conformers for the dysprosium and thulium tag resulting in two NMR signal sets for the measured protein, were not found in our case for the dysprosium, thulium and lutetium metal complexes when attached to a protein scaffold (Ln-DOTA-M8-(4*R*4*S*)-Ub^{S57C}). The three lanthanides were chosen because they displayed high (Dy, 27%), low (Tm, 9%) and negligible (Lu, 2%) of the 2nd conformer in Ln-DOTA-M8-(8*S*)-SSPy and because of their use as diamagnetic reference (lutetium) and the valuable PCS that they generate (dysprosium and thulium).

Identification of one conformational species, attachment to Ubiquitin S57C and tensor sizes and properties

All described tags show only one species in the crude product, during HPLC purification and after storage for several weeks (HPLC-ESI-MS traces in supporting information, Figures S1-S4) and only one set of signals in HSQC spectra when attached to ubiquitin S57C (Figure 2) or human carbonic anhydrase II S50C (Figure 4).

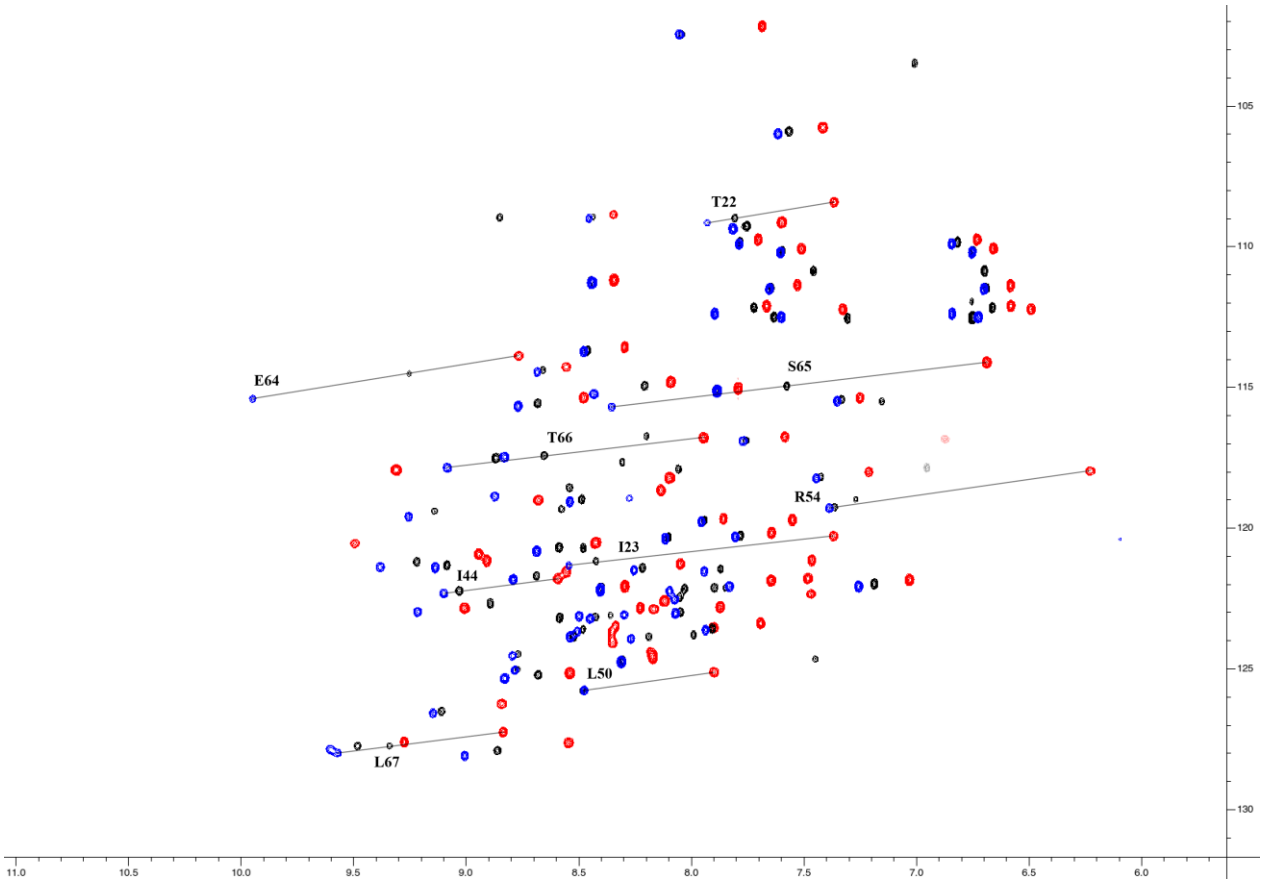

Figure 2: Overlay of ^{1}H-^{15}N HSQC spectra of Dy- (blue), Tm- (red) and Lu-DOTA-M8-(4R4S)-Ub^{S57C} (black).

Compared to DOTA-M8-(8*S*)-SSPy, the ligands in the present study display altered tensor properties (Table 1). The thulium tag offers properties well suited for the 3D structure refinement of proteins, since the combination of large axial and small rhombic tensor components results in valuable PCS independent from the orientation of the tensor to the protein if attached to a region, where the tag has a comparable flexibility as when attached to ubiquitin S57C (Figure 3). The obtained pseudocontact shifts using the thulium tag are in the range of current high-performance lanthanide chelating tags (Keizers et al. 2008; Häussinger et al. 2009; Graham et al. 2011; Peters et al. 2011; Müntener et al. 2016; Chen et al. 2018).

Table 1: Properties of the induced paramagnetic susceptibility tensors measured on ubiquitin S57C at 298K and pH 6.0.

# PCS	Ln^{3+}	$\Delta\chi_{ax}$ (10^{-32} m^3)	$\Delta\chi_{rh}$ (10^{-32} m^3)	X_{metal}	Y_{metal}	Z_{metal}	α	β	γ	Q (%)
74	Dy	-8.800	-4.167	16.809	14.475	9.226	159.079	37.736	38.477	13.7
68	Tm	19.651	2.832	16.809	14.475	9.226	174.788	44.010	82.900	6.1

The pseudocontact shifts obtained for the dysprosium lanthanide chelating tag are in a range that ensures valuable structural restraints. Furthermore, the assignment is facilitated by encountering only one set of signals. To our surprise, the dysprosium chelating tag yields smaller PCS values than the thulium tag, as a consequence of the smaller tensor parameters. This in strong contrast to the results with Ln-DOTA-M8-(8*S*)-Ub^{S57C}, where the dysprosium tag showed a

paramagnetic susceptibility tensor with considerably higher values for $\Delta\chi_{ax}$ and $\Delta\chi_{rh}$. The obtained results for Dy-DOTA-M8-(4*R*4*S*)-Ub^{S57C} could be explained by the different orientation of the sidearms of the lanthanide chelating tag (SAP or $\Lambda(\delta\delta\delta\delta)$) compared to Dy-DOTA-M8-(8*S*)-Ub^{S57C} (TSAP or $\Delta(\delta\delta\delta\delta)$). Not only are the oxygens of the carboxy groups in the (4*R*4*S*)-tag placed in the plane above the basic ring between the nitrogen atoms of the macrocycle, furthermore the dipoles of the C-O bonds of the carboxy group point in a different direction. These electronic and positional changes create a strongly different environment for the lanthanide metal and thereby significantly affect the PCS values and tensor properties as predicted by Mironov et al. (Mironov et al. 2001). Discrepancies between the classic theory of Bleaney and experimental findings are subject of current research (Bleaney 1972; Funk et al. 2015; Suturina et al. 2017).

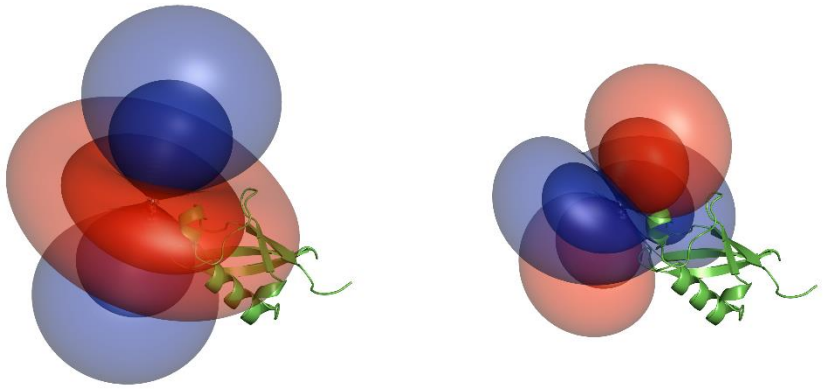

Figure 3: The tensors generated by the thulium (left) and dysprosium tag (right) and their relative orientation to ubiquitin S57C.

Surprised by the smaller tensor generated by the dysprosium tag and driven by scientific curiosity to further benchmark our lanthanide chelating tags, we decided to further validate our results on hCA II S50C.

Benchmarking on leucine labeled human carbonic anhydrase II S50C

In order to verify and confirm the tensor properties obtained for ubiquitin S57C, we tagged selectively ^{15}N leucine labeled hCA II S50C, a 29 kDa protein construct, with both the dysprosium and thulium lanthanide chelating tag.

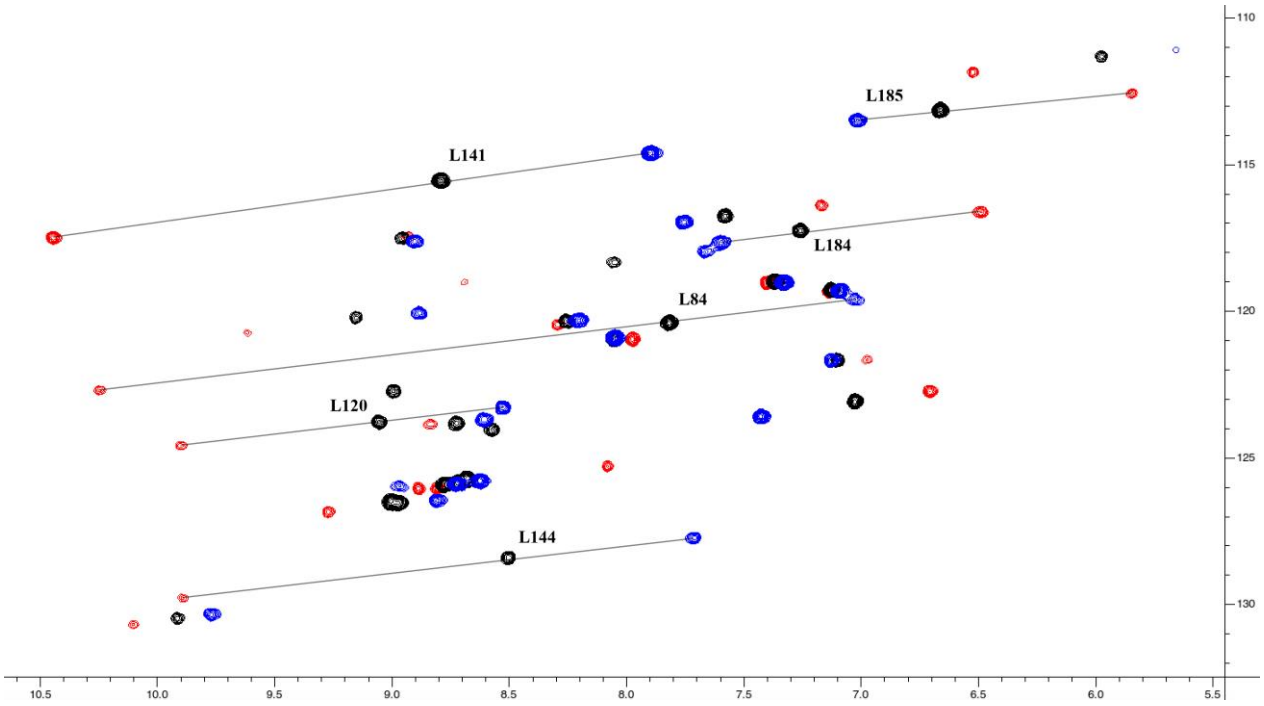

Figure 4: Overlay of ^{1}H-^{15}N HSQC spectra of Dy- (blue), Tm- (red) and Lu-DOTA-M8-(4R4S)-SSPy (black) attached to selectively ^{15}N leucine labeled hCA II S50C.

The results show that the paramagnetic susceptibility tensor generated on hCA II S50C is bigger than the tensor for ubiquitin S57C (Figure 5, Table 2). This arises most likely from a more restricted translational and/or rotational motion of the tag on the human carbonic anhydrase II. In PCS NMR spectroscopy, minor translation of the lanthanide chelating tag is tolerated, whereas rotation leads to destructive interference. Both tensor shapes and their relative magnitude when compared to each other remained the same as for ubiquitin S57C.

Table 2: Properties of the induced paramagnetic susceptibility tensors on hCA II S50C at 298K and pH 6.8.

# PCS	Ln^{3+}	$\Delta\chi_{ax}$ (10^{-32} m^3)	$\Delta\chi_{rh}$ (10^{-32} m^3)	X_{metal}	Y_{metal}	Z_{metal}	α	β	γ	Q (%)
46	Dy	-20.281	-10.505	-30.033	12.806	21.300	5.424	98.440	74.506	13.4
46	Tm	35.039	10.600	-30.033	12.806	21.300	178.943	86.884	117.477	6.9

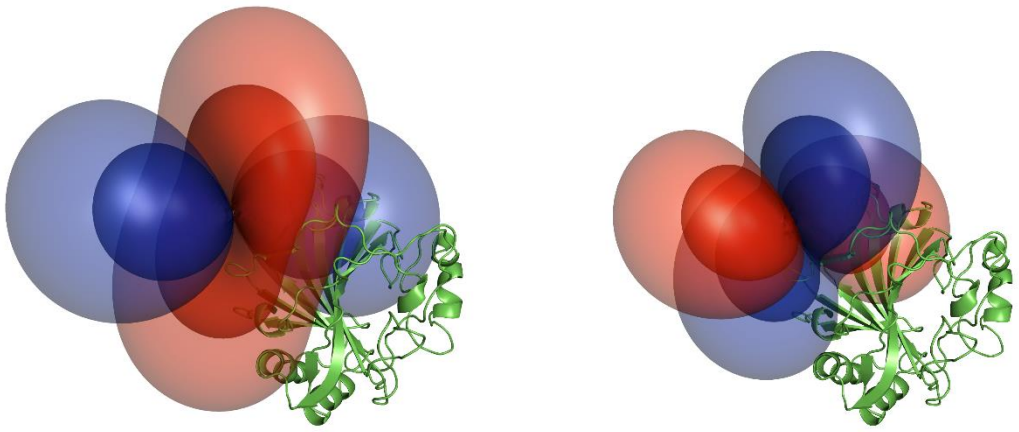

Figure 5: The tensors generated by the thulium (left) and dysprosium tag (right) and their relative orientation to human carbonic anhydrase S50C.

The orientation of both lanthanide chelating tags with regard to the protein render them ideally suitable to obtain structural restraints for studies of a protein dimer complex, in which the second protein binds in the region where the paramagnetic susceptibility tensor of the lanthanide chelating tags have their maximum impact (Figure 3 and Figure 5).

Assignment of the conformation of Lu-DOTA-M8-(4*R*4*S*)-SSPy by DFT calculations and determination of structures and stabilization energies of the two conformational species

Ranganathan et al. determined the Yb^{3+} M4-DOTMA-(4*R*4*S*) chelates to adopt SAP geometry using NMR experiments and molecular mechanics (Ranganathan et al. 2002). The experimental data and the structural assignments for the Yb^{3+} M4-DOTMA-(4*R*4*S*) chelate determined by Ranganathan et al. (Ranganathan et al. 2002) and our assignment for Lu-DOTA-M8-(4*R*4*S*)-SSPy (Häussinger et al. 2009), provided a good starting point for our conformational analysis. We performed DFT calculations to estimate the energy difference between SAP and TSAP conformers and to assign the more stable conformation for the dysprosium and thulium tag, since measuring 2D spectra of these two complexes poses insurmountable difficulties due to the extremely short T2 relaxation time caused by the close paramagnetic center (Helm 2006). The DFT calculations were performed using the BP86 functional of Becke and Perdew (Perdew 1986; Becke 1988), which shows reliable and accurate results for the comparison of energies since the errors generated by this functional occur in a mainly systematic manner, in contrast to other functionals containing empirical parameters. For example B3LYP, which can be considered as one of the most popular functionals for small organic molecules with regard to obtained results and time and effort needed (Sousa et al. 2007), was shown to perform worse than GGA functionals for lanthanide complexes and introduces increasing errors for big molecules (Redfern et al. 2000; Grimme 2005; Grimmel et al. 2016). The calculations were performed in vacuum as well as with implicit water using the CPCM solvent model, which is known to give reliable and accurate results for solvents of high polarity/dielectric constant with deviations less than 1 kcal/mol for the aqueous solvation energy of neutral molecules at B3LYP level (Takano and Houk 2005).

Table 3: Stabilization energies obtained with or without coordinated water molecule in vacuo and water solvent (L = DOTA-M8-(4R4S)-SSPy).

Calculated energies of the different complexes M(L) (E_h / Hartree)		**Stabilization (kJ/mol)**
Lu(L) TSAP	Lu(L) SAP	
-16713.85773	-16713.87043	-33.3
Lu(L) TSAP solv.	Lu(L) SAP solv.	
-16713.95067	-16713.96020	-25.0
Lu(L)·H_2O TSAP	Lu(L)·H_2O SAP	
-16790.34318	-16790.36243	-50.5
Lu(L)·H_2O TSAP solv.	Lu(L)·H_2O SAP solv.	
-16790.42518	-*	-
Tm(L) TSAP	Tm(L) SAP	
-15802.89887	-15802.90695	-21.2
Tm(L) TSAP solv.	Tm(L) SAP solv.	
-15802.98688	-15802.99067	-10.0
Tm(L)·H_2O TSAP	Tm(L)·H_2O SAP	
-15879.38336	-15879.39700	-35.8
Tm(L)·H_2O TSAP solv.	Tm(L)·H_2O SAP solv.	
-*	-*	-
Dy(L) TSAP	Dy(L) SAP	
-14504.81886	-14504.82753	-22.8
Dy(L) TSAP solv.	Dy(L) SAP solv.	
-14504.90612	-14504.91021	-10.7
Dy(L)·H_2O TSAP	Dy(L)·H_2O SAP	
-14581.30633	-14581.31911	-33.6
Dy(L)·H_2O TSAP solv.	Dy(L)·H_2O SAP solv.	
-14581.38820	-14581.39086	-7.0

-*: No converged, meaningful, nine-coordinated complex obtained in the performed DFT calculations.

Interestingly, the calculations show a stabilization towards the SAP conformer for all three metal complexes, with and without inner-shell water molecule, in vacuo and in water modeled with an implicit solvent model, with an energetic difference between the two conformers in the range of 7.0 – 50.5 kJ/mol (Table 3). The biggest stabilization towards the SAP isomer for an eight-coordinated complex in solution is obtained for the lutetium complex (25.0 kJ/mol, K = ~24000). The calculated stabilization energies for the thulium- and dysprosium complexes are smaller (10.0 kJ/mol and 10.7 kJ/mol), but still significantly exceed the thermal energy at 298 K and constitute an equilibrium constant of K = 55 and K = 76 towards the SAP conformer. The DFT optimized structures of the SAP conformers of the lutetium-, thulium- and dysprosium complexes in vacuo are depicted in Figure 6.

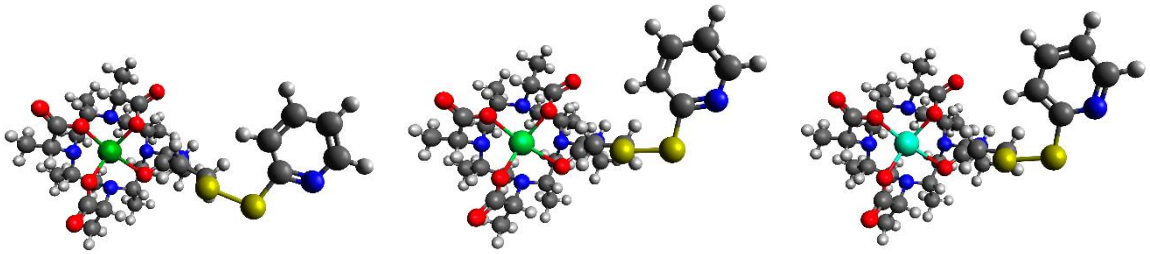

Figure 6: Structures of the SAP conformers of the lutetium-, thulium and dysprosium complexes in vacuo.

Interestingly, we did not obtain converged and meaningful 9-coordinated structures for the SAP lutetium- and thulium complexes with an inner-shell water molecule in using the CPCM solvent model. However, we observed that the inner-shell water molecule was lost to the outer-shell and aligned in a way that hydrogen bonds can be formed with the carboxylates (Figure 7). These findings from our calculations can be explained by the fact that for the smaller lanthanides ions, as thulium and lutetium, the 8-coordinated species without apical water molecule is preferred due to sterics (Benetollo et al. 2003; Strickland et al. 2016). Without solvent model (in vacuo), the water molecule stays close to the metal ion, presumably due to the interaction of the oxygen atom with the positively charged metal ion. However, using a solvent model, the water molecule is more favored to align distant from the metal ion and the interaction of the oxygen atom with the metal ion is no longer beneficial for stabilization.

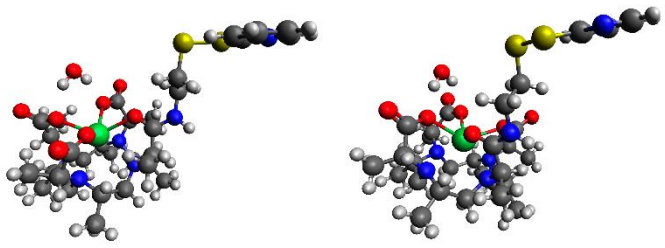

Figure 7: Eight-coordinated TSAP (left) and SAP (right) conformer of the Tm-DOTA-M8-(4R4S)-SSPy.

The SAP geometry found by Ranganathan et al. for the Yb^{3+} M4-DOTMA-(4*R*4*S*) chelates and our assignment for Lu-DOTA-M8-(4*R*4*S*)-SSPy (Häussinger et al. 2009) combined with the results of our DFT calculations clearly suggest that all lanthanide complexes presented in this work adopt a SAP (Λ(δδδδ)) geometry.

DFT calculations using other functionals and more expensive reference calculations are in progress and will be published in a separate computational study that benchmarks the accuracy and suitability of current popular and inexpensive DFT functionals used for structure and energy calculations of lanthanide complexes.

Less expensive and higher yielding synthesis

Besides the different tensor properties and suitability for PCS measurements of the thulium and dysprosium ligands presented in this study compared to their predecessor, DOTA-M8-(8*S*)-SSPy, the less expensive and higher yielding synthesis presents an important step towards the more general and routine use of the DOTA-M8-SSPy lanthanide chelating tags for the structure determination of proteins.

Conclusion

To conclude, two strongly paramagnetic lanthanide chelating tags are reported that show only one conformer and thus provide only one set of signals in HSQC experiments when attached to a protein. Furthermore, the tags show different tensor properties when attached to ubiquitin S57C compared to their DOTA-M8-(8*S*)-SSPy analog. The geometry of the lanthanide chelating tags in TSAP or SAP conformation, with and without inner-shell water molecule, in vacuo and in water modeled with a solvent model was calculated using DFT methods and the energetically most favorable conformation in all cases was assigned to be SAP. While the thulium lanthanide chelating tag is well suited for studies of the directly attached protein due to its tensor size and properties, the dysprosium tag emerges as a high-performance tag especially suited for study of a protein dimer, in which the second protein is oriented in a way that the unexploited, second tensor lobe maximally interacts. Furthermore, the comparison of Dy-DOTA-M8-(8*S*)-SSPy and Dy-DOTA-M8-(4*R*4*S*)-SSPy tag provides a starting point for further, more detailed studies on the interaction between geometry and tensor properties for lanthanide chelating tags. In order to enable studies on large proteins, protein complexes and other biopolymers, the development of high-performance lanthanide chelating tags has to be continued.

Acknowledgements

The Chemistry Department of the University of Basel and the Swiss National Science Foundation grant 200021_130263 are acknowledged for financial support. Calculations were performed at sciCORE (http://scicore.unibas.ch/) scientific computing core facility at University of Basel. Biological structures were generated using the open source software PyMOL (http://www.pymol.org/). C.E. Housecroft, E.C. Constable, T. Müntener and R. Vogel are acknowledged for helpful discussions. R.A. Byrd is gratefully acknowledged for a gift of M4-cyclen.

Conflicts of Interest

The authors declare that they have no conflict of interest.

References

Avvaru BS, Kim CU, Sippel KH, Gruner SM, Agbandje-McKenna M, Silverman DN, McKenna R (2010) A short, strong hydrogen bond in the active site of human carbonic anhydrase II. Biochemistry 49:249-251

Becke AD (1988) Density-functional exchange-energy approximation with correct asymptotic behavior. Physical Review A 38:3098-3100

Benetollo F, Bombieri G, Calabi L, Aime S, Botta M (2003) Structural Variations Across the Lanthanide Series of Macrocyclic DOTA Complexes: Insights into the Design of Contrast Agents for Magnetic Resonance Imaging. Inorganic Chemistry 42:148-157

Blahut J, Hermann P, Tosner Z, Platas-Iglesias C (2017) A combined NMR and DFT study of conformational dynamics in lanthanide complexes of macrocyclic DOTA-like ligands. Physical Chemistry Chemical Physics 19:26662-26671

Bleaney B (1972) Nuclear magnetic resonance shifts in solution due to lanthanide ions. Journal of Magnetic Resonance (1969) 8:91-100

Brewer KD, Bacaj T, Cavalli A, Camilloni C, Swarbrick JD, Liu J, Zhou A, Zhou P, Barlow N, Xu J, Seven AB, Prinslow EA, Voleti R, Häussinger D, Bonvin AMJJ, Tomchick DR, Vendruscolo M, Graham B, Südhof TC, Rizo J (2015) Dynamic binding mode of a Synaptotagmin-1–SNARE complex in solution. Nature Structural &Amp; Molecular Biology 22:555

Chen J-L, Zhao Y, Gong Y-J, Pan B-B, Wang X, Su X-C (2018) Stable and rigid DTPA-like paramagnetic tags suitable for in vitro and in situ protein NMR analysis. Journal of Biomolecular NMR 70:77-92

Cosentino U, Villa A, Pitea D, Moro G, Barone V, Maiocchi A (2002) Conformational Characterization of Lanthanide(III)−DOTA Complexes by ab Initio Investigation in Vacuo and in Aqueous Solution. Journal of the American Chemical Society 124:4901-4909

Cramer CJ, Truhlar DG (2009) Density functional theory for transition metals and transition metal chemistry. Physical Chemistry Chemical Physics 11:10757-10816

Dolg M, Stoll H, Preuss H (1993) A combination of quasirelativistic pseudopotential and ligand field calculations for lanthanoid compounds. Theoretica chimica acta 85:441-450

Dolg M, Stoll H, Savin A, Preuss H (1989) Energy-adjusted pseudopotentials for the rare earth elements. Theoretica chimica acta 75:173-194

Funk AM, Finney K-LNA, Harvey P, Kenwright AM, Neil ER, Rogers NJ, Kanthi Senanayake P, Parker D (2015) Critical analysis of the limitations of Bleaney's theory of magnetic anisotropy in paramagnetic lanthanide coordination complexes. Chemical Science 6:1655-1662

Gaponenko V, Altieri AS, Li J, Byrd RA (2002) Breaking symmetry in the structure determination of (large) symmetric protein dimers. Journal of Biomolecular NMR 24:143-148

Graham B, Loh CT, Swarbrick JD, Ung P, Shin J, Yagi H, Jia X, Chhabra S, Barlow N, Pintacuda G, Huber T, Otting G (2011) DOTA-Amide Lanthanide Tag for Reliable Generation of Pseudocontact Shifts in Protein NMR Spectra. Bioconjugate Chemistry 22:2118-2125

Grimme S (2005) Accurate Calculation of the Heats of Formation for Large Main Group Compounds with Spin-Component Scaled MP2 Methods. The Journal of Physical Chemistry A 109:3067-3077

Grimmel S, Schoendorff G, Wilson AK (2016) Gauging the Performance of Density Functionals for Lanthanide-Containing Molecules. Journal of Chemical Theory and Computation 12:1259-1266

Häussinger D, Huang J-r, Grzesiek S (2009) DOTA-M8: An Extremely Rigid, High-Affinity Lanthanide Chelating Tag for PCS NMR Spectroscopy. Journal of the American Chemical Society 131:14761-14767

Helm L (2006) Relaxivity in paramagnetic systems: Theory and mechanisms. Progress in Nuclear Magnetic Resonance Spectroscopy 49:45-64

Hikone Y, Hirai G, Mishima M, Inomata K, Ikeya T, Arai S, Shirakawa M, Sodeoka M, Ito Y (2016) A new carbamidemethyl-linked lanthanoid chelating tag for PCS NMR spectroscopy of proteins in living HeLa cells. Journal of Biomolecular NMR 66:99-110

Ikegami T, Verdier L, Sakhaii P, Grimme S, Pescatore B, Saxena K, Fiebig KM, Griesinger C (2004) Novel Techniques for Weak Alignment of Proteins in Solution Using Chemical Tags Coordinating Lanthanide Ions. Journal of Biomolecular NMR 29:339-349

Keizers PHJ, Saragliadis A, Hiruma Y, Overhand M, Ubbink M (2008) Design, Synthesis, and Evaluation of a Lanthanide Chelating Protein Probe: CLaNP-5 Yields Predictable Paramagnetic Effects Independent of Environment. Journal of the American Chemical Society 130:14802-14812

Liu W-M, Overhand M, Ubbink M (2014) The application of paramagnetic lanthanoid ions in NMR spectroscopy on proteins. Coordination Chemistry Reviews 273-274:2-12

Loh CT, Ozawa K, Tuck KL, Barlow N, Huber T, Otting G, Graham B (2013) Lanthanide Tags for Site-Specific Ligation to an Unnatural Amino Acid and Generation of Pseudocontact Shifts in Proteins. Bioconjugate Chemistry 24:260-268

Mironov VS, Galyametdinov YG, Ceulemans A, Görller-Walrand C, Binnemans K (2001) Influence of crystal-field perturbations on the room-temperature magnetic anisotropy of lanthanide complexes. Chemical Physics Letters 345:132-140

Müntener T, Häussinger D, Selenko P, Theillet F-X (2016) In-Cell Protein Structures from 2D NMR Experiments. The Journal of Physical Chemistry Letters 7:2821-2825

Natrajan LS, Khoabane NM, Dadds BL, Muryn CA, Pritchard RG, Heath SL, Kenwright AM, Kuprov I, Faulkner S (2010) Probing the Structure, Conformation, and Stereochemical Exchange in a Family of Lanthanide Complexes Derived from Tetrapyridyl-Appended Cyclen. Inorganic Chemistry 49:7700-7709

Neese F (2012) The ORCA program system. Wiley Interdisciplinary Reviews: Computational Molecular Science 2:73-78

Nitsche C, Otting G (2017) Pseudocontact shifts in biomolecular NMR using paramagnetic metal tags. Progress in Nuclear Magnetic Resonance Spectroscopy 98-99:20-49

Opina ACL, Strickland M, Lee Y-S, Tjandra N, Byrd RA, Swenson RE, Vasalatiy O (2016) Analysis of the isomer ratios of polymethylated-DOTA complexes and the implications on protein structural studies. Dalton Transactions 45:4673-4687

Otting G (2010) Protein NMR using Paramagnetic Ions. Annual Review of Biophysics 39:387-405

Pan B-B, Yang F, Ye Y, Wu Q, Li C, Huber T, Su X-C (2016) 3D structure determination of a protein in living cells using paramagnetic NMR spectroscopy. Chemical Communications 52:10237-10240

Parker D, Dickins RS, Puschmann H, Crossland C, Howard JAK (2002) Being Excited by Lanthanide Coordination Complexes: Aqua Species, Chirality, Excited-State Chemistry, and Exchange Dynamics. Chemical Reviews 102:1977-2010

Perdew JP (1986) Density-functional approximation for the correlation energy of the inhomogeneous electron gas. Physical Review B 33:8822-8824

Peters F, Maestre-Martinez M, Leonov A, Kovacic L, Becker S, Boelens R, Griesinger C (2011) Cys-Ph-TAHA: a lanthanide binding tag for RDC and PCS enhanced protein NMR. J Biomol NMR 51:329-337

Pintacuda G, Park AY, Keniry MA, Dixon NE, Otting G (2006) Lanthanide Labeling Offers Fast NMR Approach to 3D Structure Determinations of Protein−Protein Complexes. Journal of the American Chemical Society 128:3696-3702

Ramage R, Green J, Muir TW, Ogunjobi OM, Love S, Shaw K (1994) Synthetic, structural and biological studies of the ubiquitin system: the total chemical synthesis of ubiquitin. Biochem J 299 (Pt 1):151-158

Ranganathan RS, Pillai RK, Raju N, Fan H, Nguyen H, Tweedle MF, Desreux JF, Jacques V (2002) Polymethylated DOTA Ligands. 1. Synthesis of Rigidified Ligands and Studies on the Effects of Alkyl Substitution on Acid−Base Properties and Conformational Mobility. Inorganic Chemistry 41:6846-6855

Ranganathan RS, Raju N, Fan H, Zhang X, Tweedle MF, Desreux JF, Jacques V (2002) Polymethylated DOTA Ligands. 2. Synthesis of Rigidified Lanthanide Chelates and Studies on the Effect of Alkyl Substitution on Conformational Mobility and Relaxivity. Inorganic Chemistry 41:6856-6866

Redfern PC, Zapol P, Curtiss LA, Raghavachari K (2000) Assessment of Gaussian-3 and Density Functional Theories for Enthalpies of Formation of C1−C16 Alkanes. The Journal of Physical Chemistry A 104:5850-5854

Regueiro-Figueroa M, Bensenane B, Ruscsák E, Esteban-Gómez D, Charbonnière LJ, Tircsó G, Tóth I, Blas Ad, Rodríguez-Blas T, Platas-Iglesias C (2011) Lanthanide dota-like Complexes Containing a Picolinate Pendant: Structural Entry for the Design of LnIII-Based Luminescent Probes. Inorganic Chemistry 50:4125-4141

Sass J, Cordier F, Hoffmann A, Rogowski M, Cousin A, Omichinski JG, Löwen H, Grzesiek S (1999) Purple Membrane Induced Alignment of Biological Macromolecules in the Magnetic Field. Journal of the American Chemical Society 121:2047-2055

Schmitz C, Stanton-Cook MJ, Su X-C, Otting G, Huber T (2008) Numbat: an interactive software tool for fitting $\Delta\chi$-tensors to molecular coordinates using pseudocontact shifts. Journal of Biomolecular NMR 41:179

Sousa SF, Fernandes PA, Ramos MJ (2007) General Performance of Density Functionals. The Journal of Physical Chemistry A 111:10439-10452

Strickland M, Schwieters CD, Göbl C, Opina ACL, Strub M-P, Swenson RE, Vasalatiy O, Tjandra N (2016) Characterizing the magnetic susceptibility tensor of lanthanide-containing polymethylated-DOTA complexes. Journal of Biomolecular NMR 66:125-139

Su X-C, Liang H, Loscha KV, Otting G (2009) [Ln(DPA)3]3− Is a Convenient Paramagnetic Shift Reagent for Protein NMR Studies. Journal of the American Chemical Society 131:10352-10353

Su X-C, Man B, Beeren S, Liang H, Simonsen S, Schmitz C, Huber T, Messerle BA, Otting G (2008) A Dipicolinic Acid Tag for Rigid Lanthanide Tagging of Proteins and Paramagnetic NMR Spectroscopy. Journal of the American Chemical Society 130:10486-10487

Suturina EA, Mason K, Geraldes CFGC, Kuprov I, Parker D (2017) Beyond Bleaney's Theory: Experimental and Theoretical Analysis of Periodic Trends in Lanthanide-Induced Chemical Shift. Angewandte Chemie International Edition 56:12215-12218

Takano Y, Houk KN (2005) Benchmarking the Conductor-like Polarizable Continuum Model (CPCM) for Aqueous Solvation Free Energies of Neutral and Ionic Organic Molecules. Journal of Chemical Theory and Computation 1:70-77

Varghese S, Halling PJ, Häussinger D, Wimperis S (2016) High-Resolution Structural Characterization of a Heterogeneous Biocatalyst Using Solid-State NMR. The Journal of Physical Chemistry C 120:28717-28726

Vranken WF, Boucher W, Stevens TJ, Fogh RH, Pajon A, Llinas M, Ulrich EL, Markley JL, Ionides J, Laue ED (2005) The CCPN data model for NMR spectroscopy: Development of a software pipeline. Proteins: Structure, Function, and Bioinformatics 59:687-696

Wöhnert J, Franz KJ, Nitz M, Imperiali B, Schwalbe H (2003) Protein Alignment by a Coexpressed Lanthanide-Binding Tag for the Measurement of Residual Dipolar Couplings. Journal of the American Chemical Society 125:13338-13339